



# Root exudation in coastal wetlands: measuring an overlooked but significant carbon flux in mangroves

Lea Hanemann<sup>1</sup>, Huyen Thuong Dang<sup>2\*</sup>, Hermine Huot<sup>1</sup>, Cornelia Rumpel<sup>1</sup>, Lucie Maillard<sup>3</sup>, Yanni Gunnell<sup>3</sup>, Farid Dahdouh-Guebas<sup>4,5</sup>, Thi-Minh-Tam Le<sup>6,7</sup>, Nguyen The Kiet Bui<sup>8</sup>, and Marie Arnaud<sup>1</sup>

5 <sup>1</sup>Sorbonne Université, IRD, CNRS, Université Paris Cité, Univ Paris Est Créteil, INRAE, Institut d'écologie et des sciences de l'environnement de Paris, IEES, F-75005 Paris, France

<sup>2</sup>Faculty of Geology and Petroleum Engineering, Ho Chi Minh City University of Technology (HCMUT), Ho Chi Minh City, Vietnam

<sup>3</sup> Department of Geography, CNRS 5600 EVS, University Lumière Lyon 2, Bron, France

10 <sup>4</sup> Systems Ecology and Resource Management (SERM), Université libre de Bruxelles-ULB, Av. F.D. Roosevelt 50, CPi 264/1, B-1050, Brussels, Belgium

<sup>5</sup> Systems Ecology and Resource Management c/o bDIV: Ecology, Evolution & Genetics, Department of Biology, Vrije Universiteit Brussel – VUB, Pleinlaan 2 - 1050 Brussels, Belgium;

15 <sup>6</sup>Centre for Asian Research on Water (CARE), Ho Chi Minh City University of Technology (HCMUT), 268 Ly Thuong Kiet Street, D, Dien Hong Ward, Ho Chi Minh City, Viet Nam

<sup>7</sup>Vietnam National University Ho Chi Minh City, Linh Xuan Ward, Ho Chi Minh City, Viet Nam

<sup>8</sup>Management Board of Protection and Special-use Forests of Ho Chi Minh City, Ho Chi Minh City, Viet Nam

\* Correspondence to: Huyen Thuong Dang (huyen1982@hcmut.edu.vn)

20 **Abstract.** Coastal wetlands are among the most carbon-dense ecosystems on Earth, yet belowground carbon cycling remains poorly understood compared to aboveground processes. Root exudation, the release of labile organic compounds from live roots, represents a critical pathway for transferring plant-derived carbon to soils. This flux is poorly quantified because existing measurement techniques fail under flooded and tidal conditions, leaving a knowledge gap in carbon budgets. Here, we adapted and applied a sealed-cuvette system to quantify root exudation *in situ* across the two most common and

25 widespread mangrove genera worldwide (*Rhizophora* and *Avicennia*) and across contrasting wet and dry seasons in a deltaic mangrove (Cần Giò, Vietnam). The sealed cuvette method was successful in measuring root exudation, improving current methods for coastal wetlands. Mean root exudation rates were  $126 \pm 172 \mu\text{g C g}^{-1} \text{ h}^{-1}$  for *Avicennia* and  $68.5 \pm 96.1 \mu\text{g C g}^{-1} \text{ h}^{-1}$  for *Rhizophora*, with seasonal rates of  $52.4 \pm 67.2 \mu\text{g C g}^{-1} \text{ h}^{-1}$  for the wet season and  $135 \pm 168 \mu\text{g C g}^{-1} \text{ h}^{-1}$  for the dry

30 terrestrial forests. When upscaled at the ecosystem level, root exudation is estimated to represent a considerable portion of the mangrove GPP (6.1–11.9 %). We conclude that root exudation is a non-negligible and previously unaccounted-for component of mangrove carbon budgets and highlight the need for quantification of this ‘missing carbon flux’.

## 1 Introduction

Root and rhizosphere dynamics regulate belowground carbon cycling (Finzi et al., 2015; Jones et al., 2009). Yet, concealed

35 within the soil, root processes are comparatively less explored than their aboveground counterparts (Adame et al., 2024;



Wilson, 2014). In particular, root exudation is poorly quantified (Arnaud et al., 2023; Chari et al., 2024; Krüger et al., 2026). Root exudates consist, for the most part, of low-molecular-weight compounds, whose composition and rate are jointly controlled by intrinsic plant traits, including root morphology and plant developmental stage, and by extrinsic drivers including soil nutrient availability, seasonality, temperature, and soil moisture (Jones et al., 2004; Robert et al., 2025). The relative importance of these drivers is highly system- and species-specific, and their interactive effects remain poorly constrained, particularly in non-terrestrial environments (Robert et al., 2025; Vives-Peris et al., 2020).

Recent global syntheses estimate that root exudation represents approximately 7–14% of gross primary productivity (GPP) across ecosystems (Chari et al., 2024). Despite this recognised importance, exudation research has focused overwhelmingly on upland terrestrial systems, leaving root exudation in wetland soils as a particularly critical knowledge gap, especially in carbon-rich coastal wetlands like mangroves (Arnaud et al., 2023; Krüger et al., 2026). Beyond representing a direct carbon flux, root exudates may influence soil carbon dynamics in mangroves. Once released, these labile compounds influence soil carbon: either by enhancing stabilisation through organo-mineral associations or by accelerating decomposition via the priming effect (Dijkstra et al., 2021; Keiluweit et al., 2015; Panchal et al., 2022). For instance, Kato et al. (2024) showed that root exudates could stimulate dissolved inorganic carbon production and export from mangrove sediments. Quantifying root exudation is therefore essential not only to close the carbon budget, but also to understand other carbon fluxes.

Quantifying exudation remains technically challenging (Oburger and Jones, 2018), especially in coastal wetlands. Exudates occur at low concentrations, degrade rapidly, and can be reabsorbed by roots or metabolised by rhizosphere microbes (Badri and Vivanco, 2009; Oburger and Jones, 2018). Several techniques have been developed to quantify root exudation (Oburger and Jones, 2018). Among these techniques, the cuvette method (Phillips et al., 2008) offers notable advantages, as it allows exudates to be collected *in situ* from living trees with soil-grown roots while maintaining controlled sampling conditions (Williams et al., 2021). This technique was developed for terrestrial ecosystems involving i) excavation of intact root, ii) incubation of the root within an *in situ* chamber filled with a freshwater nutrient solution, iii) a settling period for root recovery from stress, and iv) extraction and measurement of dissolved organic carbon (DOC) exuded by roots (Phillips et al., 2008). Applying the cuvette method to coastal wetland systems presents challenges, as the cuvettes must remain sealed, sterile, and stable over extended periods, which is difficult to achieve in wetland environments where inundation risks leakage and/or contamination within the chamber and strong tidal currents risk damaging equipment. In addition, freshwater-based nutrient media may be unsuitable for saline wetlands. Exudation rates vary as roots recover from disturbance and as exudates accumulate or are reabsorbed, the optimal incubation duration (typically 4–72 h) must also be determined (Oburger and Jones, 2018). Consequently, direct *in situ* quantification of root exudation is rare in coastal wetlands, including mangroves (Kato et al., 2026; Krüger et al., 2026). So far, the only *in situ* measurement of root exudates using an *ad hoc* adapted cuvette method in mangroves suggested that it could represent a large portion of the ‘missing carbon’ of mangrove carbon budgets (Kato et al., 2026). Although this quantification pushed the frontier of root exudation quantification, the



70 measurements were limited to *Bruguiera gymnorhiza* in a single subtropical system and have not yet been extended to the globally dominant *Rhizophora* and *Avicennia* genera or to typical tropical mangroves, limiting the representativeness of these root exudation estimates (Kato et al., 2026). Furthermore, the reliability of wetland-adapted cuvette measurements has not yet been systematically validated under field conditions.

The aim of this study is to develop and validate the adapted sealed-cuvette method under field conditions and to quantify *in situ* root exudation rates in a typical carbon rich mangrove (Arnaud, 2020; Dung et al., 2016). We present a sealed-cuvette system adapted for *in situ* root exudate collection under the flooded, saline, and tidally dynamic conditions of mangrove soils, and describe the modifications that ensure waterproofing, contamination control, and methodological comparability with established terrestrial protocols. Our sealed cuvette system was deployed across the two most common and widespread mangrove genera worldwide (*Rhizophora* and *Avicennia*) during two consecutive seasons. We then assess the contribution of root exudation to the tropical mangrove carbon budget and explore potential drivers of exudation rates.

## 2 Methods

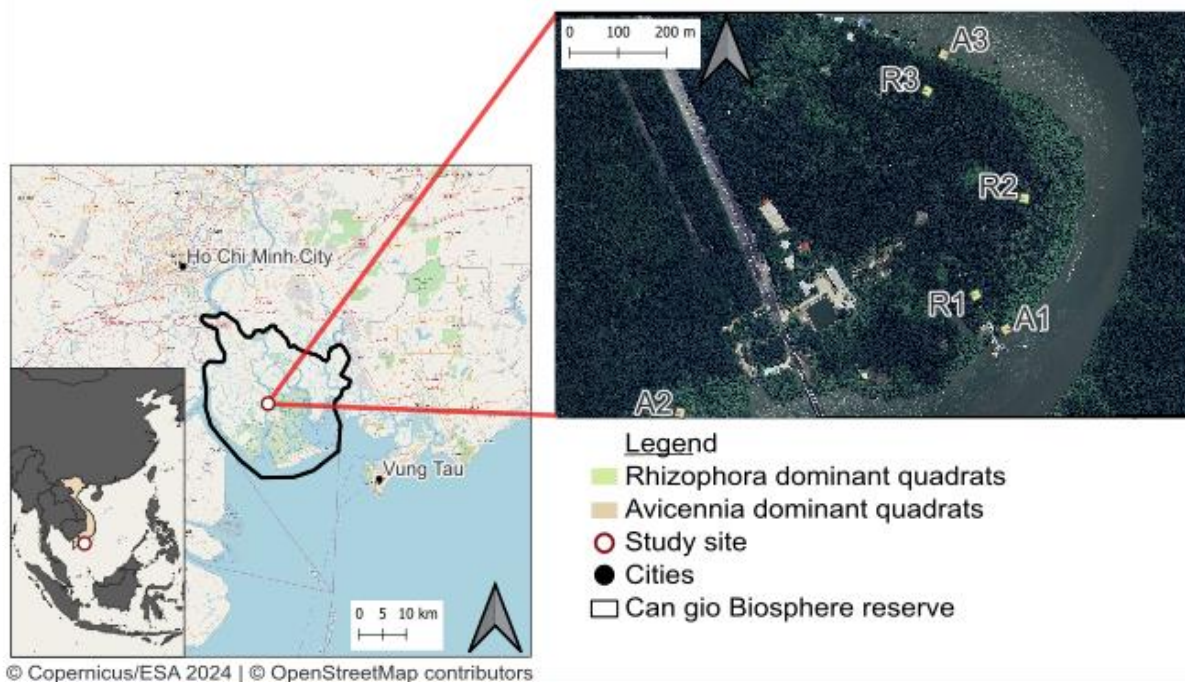
### 80 2.1 Study site

We tested and applied the sealed cuvette method in the C n Gi r Mangrove Biosphere Reserve (10 22' N, 106 54' E) during both a dry and a wet season (2024 and 2025 respectively). C n Gi r experiences a semi-diurnal tidal regime with a tidal amplitude of 2–4 m (Binh et al., 2008). The study sites were located in the core area of the C n Gi r mangrove (Fig. 1), which comprises two zones. The less inundated *Rhizophora*-dominated zone lies at 90–150 cm above mean sea level (inundation class 3; 20–45 inundations per month) and consists of planted *Rhizophora apiculata* Bl. stands established in 85 1986. The more inundated *Avicennia*-dominated zone occupies the riverside, 0–20 m from the creek at 20–30 cm above mean sea level (inundation class 2; 45–59 inundations per month) and is naturally colonised by *Avicennia alba* Bl. (Van Loon et al., 2007). Soils in both zones are clay-dominated (Arnaud, 2020) with pore-water salinity typically ranging from 16 to 30 ppt and pH varying from slightly acidic inland (6.2–6.8) to near neutral closer to the channel (Van Vinh et al., 2021). 90 Organic carbon content, sediment and particle size distribution of the C n Gi r Mangrove Biosphere Reserve are similar to other carbon rich mangroves worldwide, with total organic carbon (TOC) of ~10%, and clay content >60% (Arnaud, 2020). C n Gi r has a tropical monsoon climate (mean annual T = 25.8  C; rainfall = 1,300–1,400 mm yr<sup>-1</sup>) (Binh et al., 2008; UNESCO/MAB Project, 2000), with a wet and a dry season (Binh et al., 2008; UNESCO /MAB Project, 2000). During the wet-season campaign (8–24 August 2024), the mean temperature was 29.9  C, the relative humidity exceeded 76%, and total 95 rainfall averaged 15 mm day<sup>-1</sup>. During the dry-season campaign (24 April–1 June 2025), mean temperature was 29.6  C, relative humidity was 77%, and equivalent daily rainfall averaged 7 mm day<sup>-1</sup> (V ng T u weather station; Visual Crossing Corporation., 2024-2025).



100

105



© Copernicus/ESA 2024 | © OpenStreetMap contributors

110

**Figure 1:** Location of the study site showing the six 20 m<sup>2</sup> quadrats within the Càn Giò biosphere reserve (black line) with *Rhizophora apiculata* dominated plots (R1–R3, green) and *Avicennia alba* dominated plots (A1–A3, beige) on a true colour satellite image. Contains modified Copernicus Sentinel-2 L2A data (2024), processed by ESA. Background map data © OpenStreetMap contributors (openstreetmap.org/copyright). Maps were compiled in QGIS 3.34.8 (QGIS Development Team, (2025)) using the projection WGS 84 / UTM Zone 48 N.

## 2.2 Experimental setup

115

We established six 20 m<sup>2</sup> plots: three in *Rhizophora*-dominated stands, and three in *Avicennia*-dominated stands. We positioned the plots along three transects 300 m apart that were placed perpendicular to a tidal channel connecting the Lòng Tàu and Đòng Tranh rivers (Fig. 1). *Rhizophora*-dominated plots were located >100 m inland, while *Avicennia*-dominated plots were positioned at the riverbank. We shifted one *Avicennia* plot slightly south due to limited boat access (Fig. 1). Within each plot, we generated random points in QGIS and sampled the tree closest to each point to ensure unbiased selection. One root per tree was sampled. The number of trees sampled per treatment ranged from 5 to 21 (*Avicennia*: wet = 13, dry = 5; *Rhizophora*: wet = 21, dry = 8) due to constraints on site access caused by short tidal windows and accidental breakage of some cuvette setups due to mangrove roots being very fragile and thus easily becoming disconnected from trees.

120

We excavated fine roots within the top 30 cm of soil, and approximately 0.5–1.5 m from the trunk. Once a suitable fine root was exposed, we installed the sealed-cuvette system following the described protocol (Sect. 2.3). To compare seasons, we conducted measurements during the wet season in 2024 and repeated them during the consecutive dry season in 2025. Plot



A3 could not be correctly resampled in 2025 due to localised disturbances associated with nearby boat activity. To maintain a balanced design across species for the seasonal comparison, R3 and A3 plots were also excluded from that analysis.

## 125 2.3 Sealed-cuvette system: design and sampling protocol

### 2.3.1 Fine-root excavation and preparation

We gently excavated intact fine roots (<2 mm diameter) from live mangrove trees within the upper 0–30 cm of soil, where the depth of fine-root density is known to peak in mangroves globally (Arnaud et al., 2023) and within our study site (Arnaud et al., 2021). We selected roots with lengths of 15–20 cm, and with healthy colour and turgidity. We removed  
130 adherent sediment from the roots and rinsed them with a carbon-free saline solution prepared from Instant Ocean® Sea salt (Fig. 2.a). This solution replicates coastal porewater major-ion composition (McIver et al., 2023), and the dilution was adjusted to match local porewater salinity, exposing the root to chemically familiar conditions and preventing abrupt shifts in ionic strength during handling.

### 2.3.2 Cuvette assembly

We enclosed the exposed fine roots in a sterile polypropylene syringe (30 mL; Terumo Corp., Tokyo, Japan) that served as the cuvette body (Fig. 2.a). We filled the syringe with acid-washed glass beads (Acros Organics, Thermo Fisher Scientific, Illkirch, France) to recreate soil mechanical impedance and maintain root–substrate contact (Lopez-Guerrero et al., 2022). In the wet season, we used a layered combination of fine (750 µm) and coarse (4 mm) beads to avoid valve clogging; in the dry season, due to logistical constraints (i.e. availability), we used a uniform 2 mm bead size. Substrate particle size is not  
140 assumed to affect exudation quality (Sasse et al., 2020). We sealed each syringe with one or two rubber stoppers containing a small incision for root passage. These stoppers create an airtight seal around the root and stabilise it within the cuvette. We placed a three-way stopcock (VWR International, USA) at the base to allow flushing with saline solution and subsequent sampling (Fig. 2.b). We flushed each cuvette with 30 mL of saline solution in three 10 mL increments to remove contaminants, after which we injected 5–10 mL of solution into the cuvette to maintain moist, porewater-like conditions  
145 around the roots. All components were sterilised prior to use and handled aseptically to minimize contamination.

### 2.3.3 Waterproof housing

We replaced the valve with a sterile stopper and placed the entire cuvette in a vacuum-sealed polyethylene bag (Aigostar, Irvine, CA, USA) and placed this within a hermetic junction box (Restmo, Boston, MA, USA) sealed using aquarium-grade silicone sealant (AquaSil Transparent; JBL, Neuhofen, Germany) (Fig. 2.c). We partially buried the cuvette housing to  
150 maintain a stable temperature and stabilise the set-up against the tide. When tidal currents were stronger, as was the case in our study sites in the dry season, we reinforced the seals with plastic wrap and stabilised the housing with wire arches.



### 2.3.4 Incubation protocol and exudate recovery

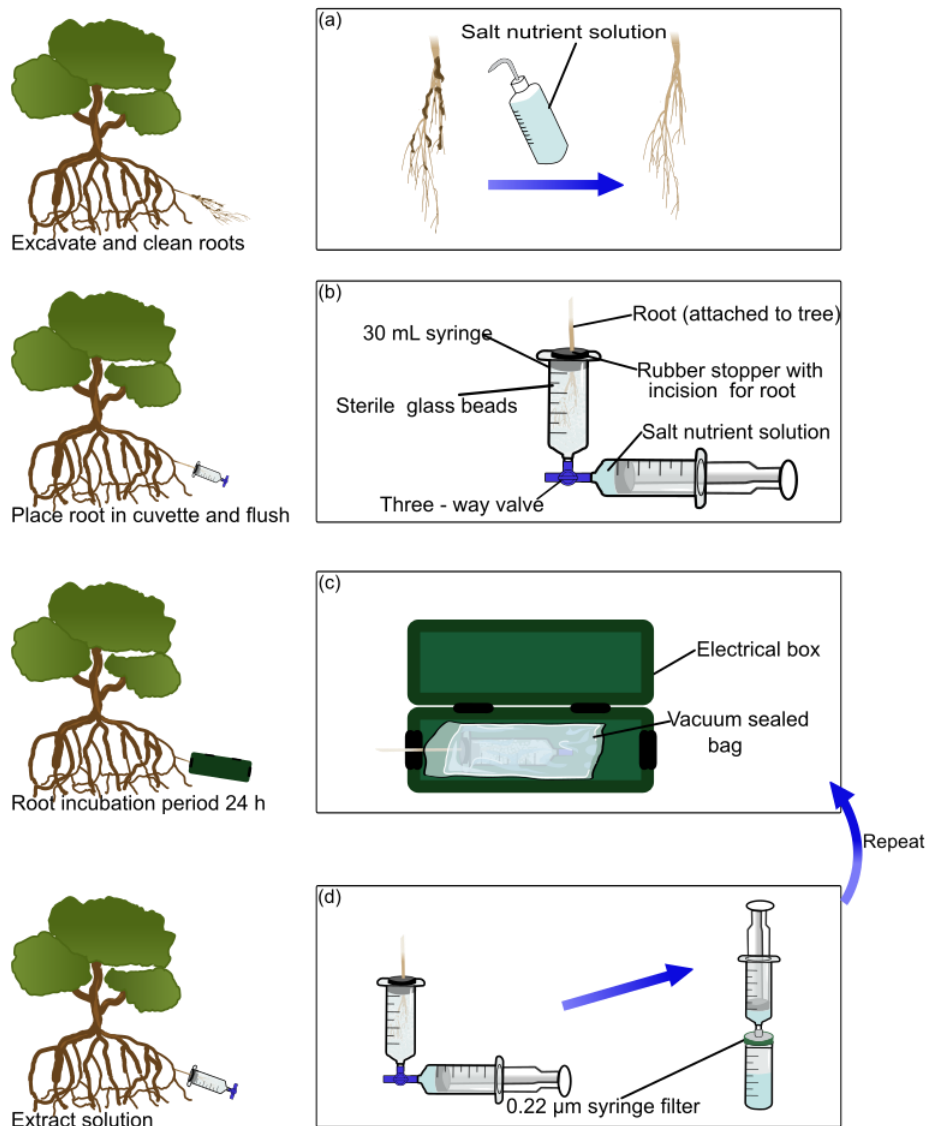
155 Following installation, we left the enclosed roots for a 24 h incubation recovery period to allow physiological stabilisation after excavation (see Sect. 3.2 and 4.1 for the validation of this choice). Then, we extracted the cuvette from the waterproof set-up and replaced the three-way valve. We collected the 5–10 mL of solution retained in the cuvette during the recovery period and then flushed the cuvette with additional saline solution until we recovered a total volume of 30 mL. Then we added 5–10 mL of fresh saline solution and incubated the cuvette for a further 24 h as above. At the end of the second 24 h incubation (48 h total), we again collected 30 mL of solution (Fig. 2.d). We passed the recovered solution through a 0.22  $\mu\text{m}$  PVDF syringe filter (Millex; MilliporeSigma, Burlington, MA, USA), collected it in sterile Falcon™ polypropylene tubes (Corning Inc., Corning, NY, USA), wrapped them in aluminium foil, and stored them at 4 °C for up to 7 days before DOC analysis.

### 2.3.5 Post-incubation root harvesting

After collecting the final dose of solution, we excised the enclosed root near the syringe tip, wrapped it in Parafilm and aluminium foil, and stored it at 4 °C for subsequent functional-trait and biomass analyses (Sect. 2.5.2).

### 165 2.3.6 Controls

To correct for background DOC unrelated to root activity, we included two root-free control cuvettes in each quadrat processed in parallel with sample cuvettes. We blank-correct DOC concentrations measured by subtracting the mean DOC concentration of the two corresponding quadrat controls before calculating exudation rates. In the dry season, only two control cuvettes were measured, and a single pooled blank mean was applied to all dry-season samples.



170

Figure 2: Experimental system for sealed cuvette *in situ* exudate collection from fine mangrove roots. Panels (a–d) show the sequence of operations: (a) Root excavated, cleaned and flushed with salt-nutrient solution, remaining attached to the parent tree. (b) Root placed in a 30 mL syringe packed with salt-nutrient solution and acid-washed glass beads (750  $\mu\text{m}$  and 4 mm) and sealed with a rubber septum. (c) Cuvette vacuum-bagged and enclosed within a waterproof electrical junction box, sealed with silicone and then partially buried at the sampling point. (d) Cuvette flushed with salt-nutrient solution at 0, 24 and 48 hours; exudate drawn off through the septum, passed through a sterile 0.22  $\mu\text{m}$  syringe filter, and collected for analysis.

175



## 2.4 Sealed-cuvette system validation

### 2.4.1 Waterproofing under laboratory and tidal conditions

180 We tested the watertightness of the sealed-cuvette system in both the laboratory and the field. In the laboratory, we assembled three full cuvettes following the protocol described above and used a 2 mm cotton string to simulate the diameter and flexibility of a fine mangrove root. We set up the cuvettes as described (Sect. 2.2) and fully submerged them for 24 h to assess sealing performance under water. For the *in situ* pilot, we excavated three fine roots and installed them in sealed cuvettes. In the same plot (R1), we also deployed three root-free control cuvettes. We buried all six cuvettes *in situ* and left them in place for 72 h to test waterproofing under tidal conditions.

### 185 2.4.2 Optimisation of incubation duration

To determine a suitable recovery and incubation period, we conducted an *in situ* time series using the sealed-cuvette protocol and sampled solutions from the same three roots used in the field waterproof test at 0, 24, 48, and 72 h. These intervals span a full diurnal cycle of exudation, which has been shown to fluctuate significantly over 24 h, and suggests a mechanistic link between the supply of newly assimilated photosynthates and root exudates (Brauner et al., 2018; Tixier et al., 2023). Shorter incubations were also not feasible due to the operational constraints imposed by tidal access. The chosen duration also reflects the methodological guidance that exudate collection must balance sufficient solute accumulation against the increasing risk of microbial degradation and reuptake during longer exposures (Oburger and Jones, 2018).

## 2.5 Fine-root biomass and trait quantification

### 2.5.1 Fine root biomass

195 We quantified fine-root biomass density in the wet season using soil cores (diameter: 4.2 cm; depth: 30 cm). Roots were washed from each core and separated by diameter ( $>2$  mm,  $<2$  mm) and by condition (live vs dead) following Freschet et al. (2021). Each fraction was oven-dried at 60 °C for 48 h and weighed using an analytical balance (HT 224 HT Series; readability 0.1 mg; A&D Company Ltd., Tokyo, Japan). Fine-root biomass density ( $\text{g cm}^{-3}$ ) was calculated as the dry mass of live roots  $< 2$  mm divided by the soil-core volume.

### 200 2.5.2 Root morphological and functional trait analysis

Roots collected from the sealed cuvettes were processed for trait measurements and for determining the dry mass needed to calculate exudation rates. After removing glass beads, each root was spread out in a thin water layer in a transparent tray and scanned using a flatbed scanner (Scanjet G3110; Hewlett-Packard, Palo Alto, CA, USA; 600 dpi). The resulting images were analysed using WinRHIZO Pro 2007 (Regent Instruments, Québec, Canada) to obtain total root length, surface area, and volume. We classified roots into fine ( $<0.8$ , 0.8 - 1.0, 1.0 - 1.2 and 1.2 - 2 mm) and coarse ( $>2$  mm) fractions. Specific root



length (SRL,  $\text{cm g}^{-1}$ ) was calculated as the total length of fine roots divided by their dry mass. Root tissue density (RTD,  $\text{g cm}^{-3}$ ) was calculated as the dry mass of fine roots divided by their total volume. After scanning, the roots were oven-dried at  $60^\circ\text{C}$  for 48 h and weighed to obtain the dry mass used in exudation-rate calculations.

## 2.6 Dissolved organic carbon analysis

210 We analysed the collected exudate samples using a TOC analyser (TOC-L; Shimadzu Scientific Instruments, Columbia, MD, USA). Prior to sample analysis, the instrument was calibrated following the manufacturer's protocol. Analytical performance was verified by running a certified organic carbon reference material (CRM Cat. #669) and Milli-Q water blanks to assess baseline stability and instrument response. Standard solutions and blanks were measured periodically throughout the analysis sequence to confirm continued calibration validity. We blank-corrected all DOC data using DOC from root-free cuvettes and  
215 removed any negative value. Exudation rates were calculated as:

$$\text{Exudation rate } (\mu\text{g C g}^{-1} \text{ h}^{-1}) = \frac{(\text{Total } C_{\text{sample}} - \text{Total } C_{\text{control}})}{M_{\text{root}} \times t_{\text{incubation}}} \quad (1)$$

where  $\text{Total } C_{\text{sample}}$  and  $\text{Total } C_{\text{control}}$  are the total DOC in the sample and the control cuvettes (in  $\mu\text{g C}$ ), calculated as DOC concentration (in  $\mu\text{g L}^{-1}$ )  $\times$  solution volume (in L);  $M_{\text{root}}$  is the dry mass of fine roots (in g) collected from the cuvette; and  $t_{\text{incubation}}$  is the incubation duration (i.e., 24 h).

## 220 2.7 Upscaling to ecosystem-level carbon fluxes

We multiplied fine-root exudation rates ( $\mu\text{g C g}^{-1} \text{ h}^{-1}$ ) by the root biomass density ( $\text{g cm}^{-3}$ ) to obtain volumetric fluxes ( $\text{mg C cm}^{-3} \text{ h}^{-1}$ ). These values were converted to annual areal fluxes using:

$$\text{Flux } (\text{kg C ha}^{-1} \text{ yr}^{-1}) = \frac{\text{Exudation rate} \times \text{root biomass} \times 24 \times 365}{10^5} \quad (2)$$

225 where exudation rate is in  $\mu\text{g C g}^{-1} \text{ h}^{-1}$  and root biomass is quadrat level fine-root biomass ( $\text{g m}^{-2}$ ), derived from soil cores (30 cm depth) as fine-root density ( $\text{g cm}^{-3}$ )  $\times$   $300,000 \text{ cm}^3$  (the volume of  $1 \text{ m}^2$  to 30 cm depth), assuming uniform vertical root distribution. The constants 24 and 365 convert the hourly rate to an annual flux, and the denominator  $10^5$  accounts for unit conversion ( $\mu\text{g}$  to  $\text{kg}$ :  $\div 10^9$ ;  $\text{m}^2$  to  $\text{ha}$ :  $\times 10^4$ ).

## 2.8 Soil analyses

### 2.8.1 Topsoil physicochemical characterisation

230 To characterise edaphic conditions, we collected one topsoil sample ( $\sim 100 \text{ g}$ ) adjacent to each excavated root. The samples were freeze-dried, disaggregated in a sterilised mortar and pestle, and sieved to  $< 2 \text{ mm}$ . A  $10\text{--}20 \text{ g}$  subsample was milled to  $< 150 \mu\text{m}$  and analysed for soil pH and electrical conductivity (EC) in 1:5 (w/v) soil–water suspensions using a pH electrode



(InLab Expert Go-ISM; Mettler Toledo, Switzerland) and conductivity meter (ProfiLine Cond 3310; Xylem Analytics WTW, Germany).

## 235 2.8.2 Soil bulk density measurement

We measured bulk density by collecting three replicate soil cores from the topsoil in each quadrat (5 cm depth × 4.9 cm diameter). For each core, we oven-dried samples at 105 °C to constant mass. Bulk density (BD, g cm<sup>-3</sup>) was calculated as oven-dry mass divided by total core volume.

## 2.9 Statistical analysis

240 To compare total carbon recovered between root cuvettes and blank controls, we used the Wilcoxon rank-sum test (Mann–Whitney U), as data were right-skewed with unequal group sizes. For the incubation duration test, we applied Friedman's test to assess the overall effect of time across the four sampling time-points, followed by Holm–Bonferroni-corrected pairwise Wilcoxon signed-rank tests. Paired measurements at 24 h and 48 h were then compared using a paired Wilcoxon signed-rank test. Agreement between the two incubation durations was quantified using Lin's concordance correlation coefficient (CCC; 245 Lin, 1989), which simultaneously captures both precision and accuracy, unlike Pearson's r alone.

To compare root exudation rates between seasons and species, we used Gamma generalised linear models (GLMs) with a log link function, which are well-suited to continuous positive, right-skewed data. Species or season was included as a covariate in each respective model to control for confounding effects, and we also tested for a species × season interaction. Model fit was assessed using Nagelkerke's R<sup>2</sup> and dispersion ratios via DHARMA residual diagnostics. Estimated marginal means 250 (EMMs) and pairwise contrasts were reported on the response scale as ratios with 95% confidence intervals.

For comparisons of root traits (specific root length and root tissue density) and soil properties (pH, electrical conductivity and bulk density) between species and seasons, we applied Student's t-tests, Welch's t-tests, or Wilcoxon rank-sum tests depending on the outcome of normality and variance checks. Effect sizes for Wilcoxon tests were quantified as rank-biserial correlation coefficients. Spearman correlations were used to explore relationships between root exudation rates and root 255 traits, soil properties, and climatic and stand structure variables (Appendix A). Principal component analysis (PCA) was performed to visualise multivariate patterns in root traits, soil properties, climatic variables, and stand structure across species and seasons. Statistical significance was set at  $\alpha = 0.05$  for all tests. All analyses were conducted in R (version 4.4.1; R Core Team, 2024) using RStudio (Posit Team, 2024) and the packages glmmTMB, emmeans, effectsize, DescTools, BSDA, car, DHARMA, rstatix, FactoMineR, factoextra, ggcorrplot, ggrepel, ggpubr, cowplot, and flextable.

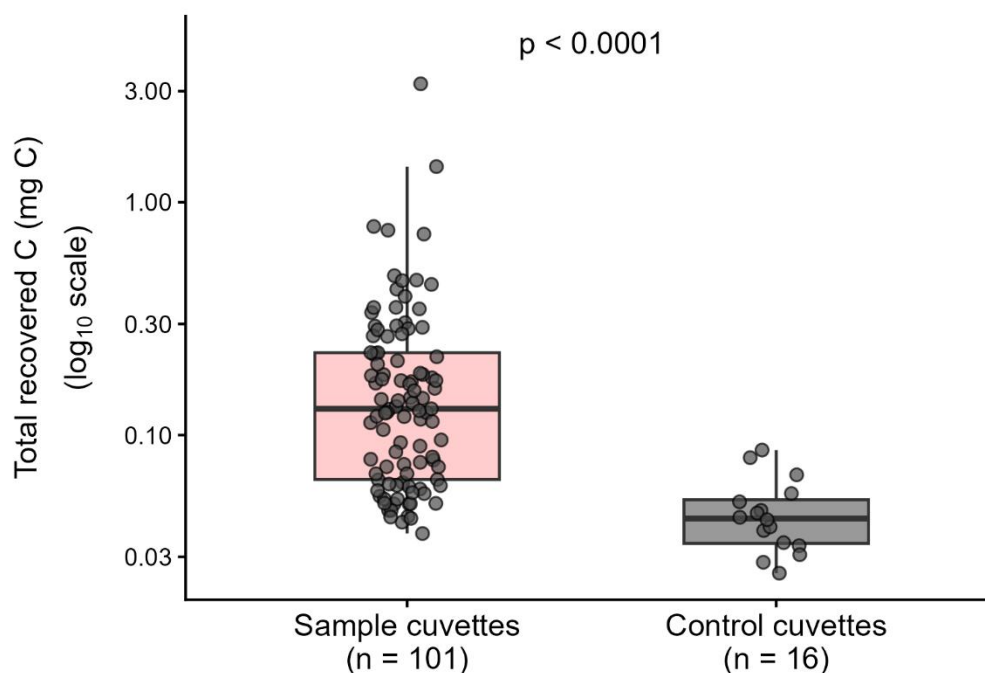


## 260 3 Results

### 3.1 Sealed-cuvette waterproofing performance under laboratory and field conditions

Laboratory submersion tests showed that all three assembled cuvettes remained watertight during 24 h of continuous immersion; the vacuum-sealed bag remained dry, and no fluid entered the cuvette body. In the field pilot, all sealed cuvettes deployed under tidal conditions remained intact over the 72 h test period. None of the cuvettes with roots (zero leakage, n = 3) or the controls (zero leakage, n = 3) showed visible leakage or water ingress when retrieved.

265 Across all sampling campaigns, 101 root cuvettes and 16 blank control cuvettes were analysed. Total C recovered from root cuvettes was consistently higher than in blanks (Fig. 3). Root cuvettes showed a median total C of 0.130 mg C (interquartile range (IQR): 0.161; range: 0.0378–3.225 mg C; n = 101), whereas control cuvettes showed a median of 0.0438 mg C (IQR: 0.0185; range: 0.0255–0.0862 mg C; n = 16). A significant difference in total C was detected between root cuvettes and  
270 controls (Wilcoxon rank-sum test:  $W = 1474$ ,  $p = 1.3 \times 10^{-7}$ ).



275 **Figure 3: Total carbon in sample and control cuvettes.** Total recovered carbon (mg C) was measured from root cuvettes (n = 101) and non-root control cuvettes (n = 16). Boxplots show the median (horizontal bar), interquartile range (IQR box) with whiskers extending to  $1.5 \times$  IQR; individual samples are overlaid as points. There is a significant difference in measured carbon between groups (Wilcoxon rank-sum test  $p = 1.3 \times 10^{-7}$ ).

### 3.2 Optimisation of incubation duration under field conditions

Mean exudation rate rose from  $6.81 \pm 7.63$  SD  $\mu\text{g C g}^{-1} \text{h}^{-1}$  at 0 h to  $32.20 \pm 12.74$  SD  $\mu\text{g C g}^{-1} \text{h}^{-1}$  at 24 hours, and peaked at  $56.19 \pm 46.31$  SD  $\mu\text{g C g}^{-1} \text{h}^{-1}$  at 48 hours, then declined to  $17.55 \pm 7.68$  SD  $\mu\text{g C g}^{-1} \text{h}^{-1}$  at 72 hours (n = 3; Fig. 4).



280 Incubation time had a significant overall effect ( $\chi^2(3) = 8.20, p = 0.042$ ), but post-hoc tests showed no significant pairwise differences (in all cases  $p = 1.00$ ).

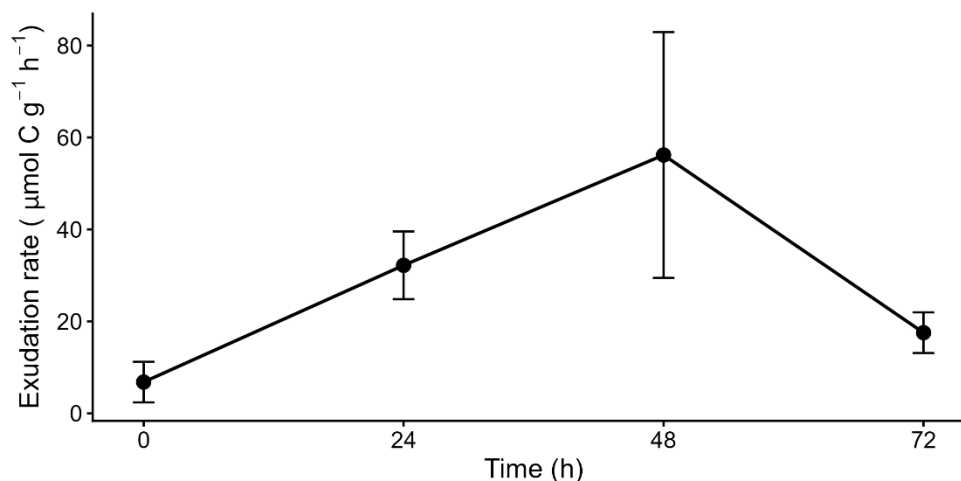
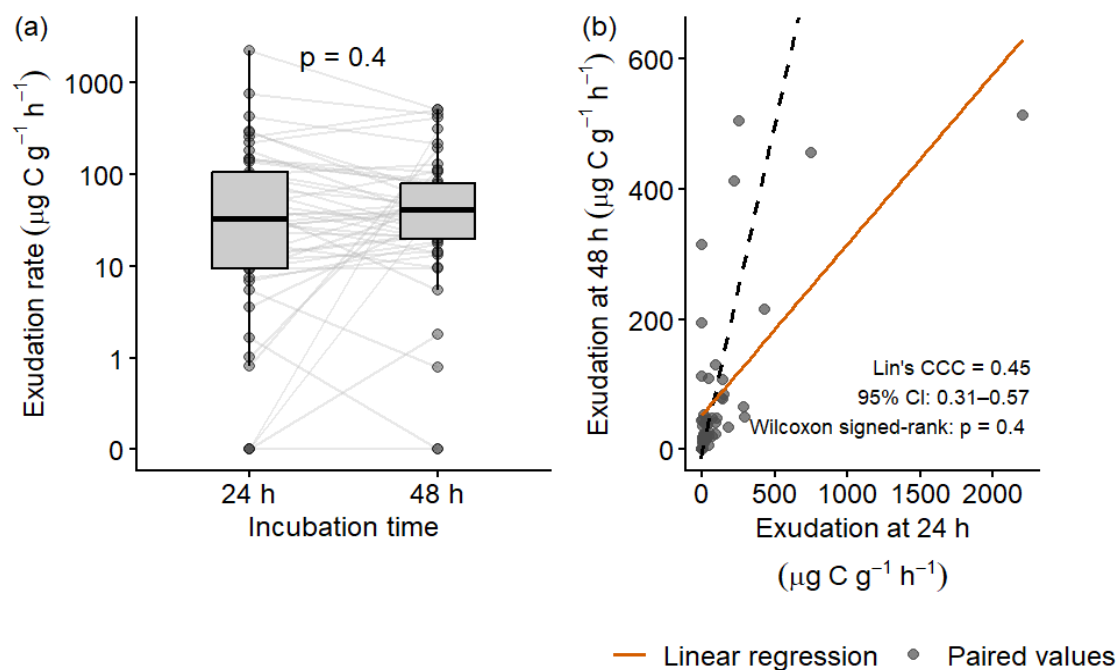


**Figure 4:** Time course of exudation rate from excised mangrove roots in a pilot time-series trial. Exudation rates ( $\mu\text{g C g}^{-1} \text{h}^{-1}$ ) were measured at 0, 24, 48 and 72 h ( $n = 3$  per time point). Points denote mean values and error bars represent  $\pm$  standard error (SE).

285 Paired measurements ( $n = 49$ ) showed median exudation of  $32.7 \mu\text{g C g}^{-1} \text{h}^{-1}$  at 24 h (IQR: 96.8) and  $40.8 \mu\text{g C g}^{-1} \text{h}^{-1}$  at 48 h (IQR: 59.6). There was no significant difference between the two incubation durations ( $V = 506, p = 0.40$ ). A distribution-free sign test gave consistent results ( $S = 23, p = 0.89$ ), with a median paired difference of  $-0.46 \mu\text{g C g}^{-1} \text{h}^{-1}$  (95% CI:  $-22.3$  to  $9.2$ ). Agreement between 24 h and 48 h measurements, quantified using Lin's concordance correlation coefficient, was poor (CCC = 0.45, 95% CI: 0.31–0.57; Fig. 5; Lin, 1989).

290



295

**Figure 5:** Comparison of paired exudation measurements at 24-hour and 48-hour incubation durations. (a) Boxplots show exudation rates ( $\mu\text{g C g}^{-1} \text{h}^{-1}$ ) at 24 h and 48 h. Individual paired measurements ( $n = 49$ ) are shown as connected grey lines. Boxes denote median and interquartile range; whiskers extend to  $1.5 \times \text{IQR}$ . No significant difference was detected between durations (paired Wilcoxon signed-rank test  $p = 0.4$ ). (b) Scatterplot of paired 24 h vs. 48 h measurements showing agreement between incubation durations. Dashed line represents 1:1 correspondence; orange line shows linear regression.

### 3.3 Mangrove root exudation rates

#### 3.3.1 Seasonal variation in root exudation

Root exudation rates measured during the wet season ( $n = 22$ ) yielded a raw mean of  $52.4 \mu\text{g C g}^{-1} \text{h}^{-1}$  (median = 30.6, range = 9.39–314.65) compared to the dry season ( $n = 10$ ) with a raw mean of  $135.0 \mu\text{g C g}^{-1} \text{h}^{-1}$  (median = 48.4, range = 9.47–455.06; Fig. 6). The model-estimated marginal means (EMMs) were  $59.9 \pm 12.7 \text{ SE } \mu\text{g C g}^{-1} \text{h}^{-1}$  for the wet season and  $103.3 \pm 30.8 \text{ SE } \mu\text{g C g}^{-1} \text{h}^{-1}$  for the dry season, representing a non-significant 1.72-fold increase during the dry season (95% CI: 0.81–3.69,  $z = 1.40$ ,  $p = 0.16$ ). The model explained 41% of the variance (Nagelkerke  $R^2 = 0.41$ ) with no evidence of overdispersion (dispersion ratio = 1.64,  $p = 0.27$ ).

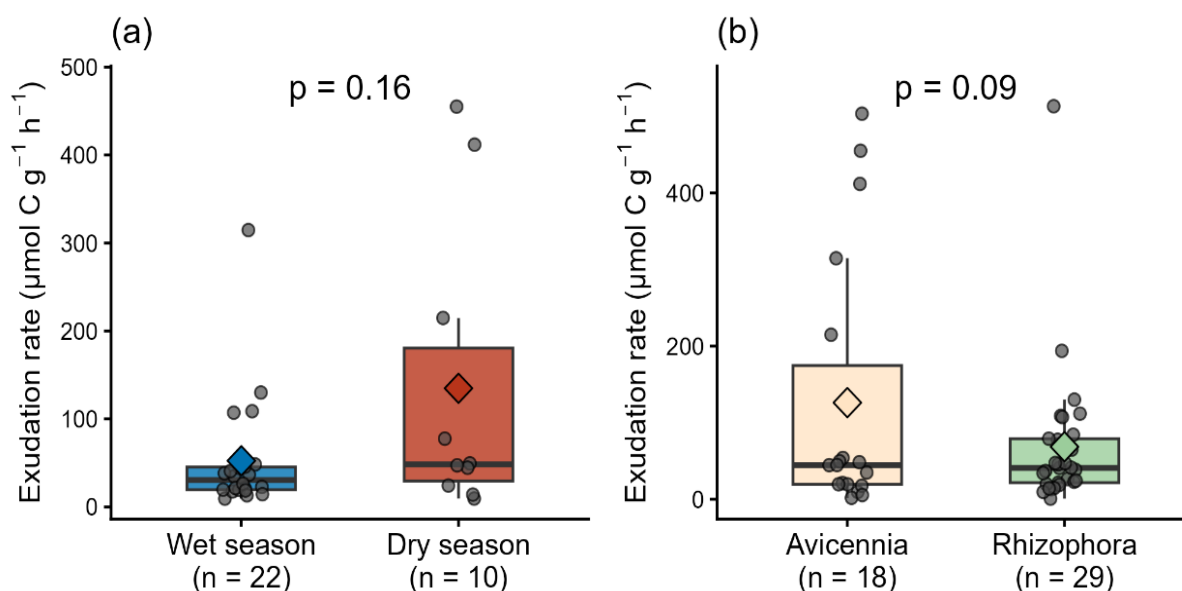
#### 3.3.2 Inter-specific variation in root exudation

Root exudation in *Avicennia* ( $n = 18$ ) showed raw means of  $126 \mu\text{g C g}^{-1} \text{h}^{-1}$  (median = 44.4, range = 1.73–503.46) and *Rhizophora* exudation rates ( $n = 29$ ) showed raw means of  $68.5 \mu\text{g C g}^{-1} \text{h}^{-1}$  (median = 40.8, range = 0.69–513.22 Fig. 6). After controlling for seasonal effects using a Gamma GLM, the estimated marginal means ( $\pm \text{SE}$ ) were  $134.8 \pm 35.1 \mu\text{g C g}^{-1} \text{h}^{-1}$  for *Avicennia* and  $78.4 \pm 17.1 \mu\text{g C g}^{-1} \text{h}^{-1}$  for *Rhizophora* (ratio = 1.72, 95% CI: 0.91–3.23,  $z = 1.68$ ,  $p = 0.093$ ). A

305



310 model including a season  $\times$  species interaction term was not significant ( $\chi^2 = 0.25$ ,  $p = 0.62$ ). The model explained 27% of  
the variance ( $R^2 = 0.27$ ) with no evidence of overdispersion (dispersion ratio = 1.22,  $p = 0.49$ ).



315 **Figure 6: Root exudation rates across species and seasons in C n Gi  mangrove.** Root exudation rates ( $\mu\text{g C g}^{-1} \text{h}^{-1}$ ) from 48-hour  
incubations in *Avicennia alba* and *Rhizophora apiculata*. (A) Seasonal comparison from plots 1 and 2 only (wet season:  $n = 22$ ; dry  
season:  $n = 10$ ). (B) Species comparison across both seasons and all plots (A:  $n = 18$ ; R:  $n = 29$ ). Boxplots show median (centre  
line), interquartile range (box), and  $1.5 \times$  IQR (whiskers). Individual measurements are shown as grey circles; filled diamonds  
indicate raw arithmetic means. P-values from estimated marginal means (EMMs) contrasts are shown above each panel. EMMs  
were derived from Gamma generalized linear models (GLMs) with log link: (A) controlling for season effect; (B) controlling for  
species effect. Neither seasonal (ratio = 1.72, 95% CI: 0.81–3.69,  $p = 0.16$ ) nor species (ratio = 1.72, 95% CI: 0.91–3.25,  $p = 0.093$ )  
320 differences were statistically significant.

325



### 3.4 Fine-root biomass and trait quantification

#### 3.4.1 Fine-root biomass

330 Fine-root biomass in the wet season averaged  $275.8 \pm 197.3 \text{ g m}^{-2}$  for *Avicennia* ( $n = 9$ ) and  $198.5 \pm 150.2 \text{ g m}^{-2}$  for *Rhizophora* ( $n = 9$ ; Table 1). Both species showed substantial within-group variability.

**Table 1. Fine-root biomass by species (wet season only).**

		Wet season <sup>b</sup>
Species	n	Fine-root biomass ( $\text{g m}^{-2}$ ) <sup>a</sup>
<i>Avicennia</i>	9	$275.8 \pm 197.3$ (110.1–554.0)
<i>Rhizophora</i>	9	$198.5 \pm 150.2$ (22.5–389.6)

<sup>a</sup>Values shown as mean  $\pm$  standard deviation (range). Fine-root biomass (live roots  $< 2 \text{ mm}$  diameter) was measured from soil cores (4.2 cm diameter, 30 cm depth), wet season only. <sup>b</sup>Dry-season biomass values were anomalously high and are

335 likely a sampling artefact; they are therefore excluded here and from ecosystem-scale flux calculations.

#### 3.4.2 Root morphological and functional trait analysis

Results of cuvette root morphology are summarised in Table 2. RTD was significantly higher in *Rhizophora* than *Avicennia* ( $W = 144$ ,  $p = 0.011$ ,  $r = -0.45$ ) and higher in the dry season than the wet season ( $W = 110$ ,  $p = 0.009$ ,  $r = -0.50$ ). SRL was  
340 higher in the wet season than the dry season ( $W = 336$ ,  $p = 0.006$ ,  $r = 0.52$ ) but did not differ between species ( $W = 313$ ,  $p = 0.260$ ). Fine roots smaller than 0.8 mm consistently dominated the sampled root pool, accounting for 86–94% of total root length across all species and season combinations.

345



**Table 2. Root trait summary by species and season.**

Species	Season	n	Root traits		Root length by diameter class (%)				
			RTD (g cm <sup>-3</sup> ) <sup>a</sup>	SRL (m g <sup>-1</sup> ) <sup>a</sup>	<0.8 mm	0.8–1.0 mm	1.0–1.2 mm	1.2–2.0 mm	>2.0 mm
<i>Avicennia</i>	Wet	13	0.101 ± 0.048 (0.110)	155.1 ± 250.3 (63.5)	90.0	2.7	1.4	2.7	3.2
<i>Avicennia</i>	Dry	5	0.126 ± 0.048 (0.135)	36.7 ± 26.4 (31.5)	86.3	1.8	2.3	6.7	2.9
<i>Rhizophora</i>	Wet	21	0.227 ± 0.321 (0.132)	56.5 ± 23.0 (59.1)	89.8	2.7	1.5	2.8	3.1
<i>Rhizophora</i>	Dry	8	0.252 ± 0.142 (0.199)	38.8 ± 23.8 (42.9)	93.5	1.3	0.9	3.0	1.2

<sup>a</sup>Values shown as mean ± standard deviation (median). RTD = root tissue density; SRL = specific root length. RTD differed significantly between species ( $W = 144, p = 0.011, r = -0.45$ ) and seasons ( $W = 110, p = 0.009, r = -0.50$ ). SRL differed between seasons ( $W = 336, p = 0.006, r = 0.52$ ) but not species ( $W = 313, p = 0.260$ ).

### 3.5 Soil analysis

#### 3.5.1 Topsoil physicochemical properties

Results are summarised in Table 3. Soils were acidic, moderately to highly saline and bulk density low. Soils beneath *Avicennia* had higher pH ( $t_{45} = 2.55, p = 0.014$ ) and EC ( $t_{45} = 2.23, p = 0.031$ ) than soils beneath *Rhizophora*, but lower bulk density ( $W = 87, p < 0.001, r = -0.67$ ). Soil pH did not differ between seasons ( $p = 0.91$ ). EC was higher in the dry season ( $W = 130, p = 0.031$ ), as was bulk density ( $W = 95, p = 0.003, r = -0.57$ ).



**Table 3. Soil properties adjacent to sampled roots by species and season.**

Species	Season	n	Soil properties		
			pH <i>Sp</i> *   <i>Se</i> ns	EC (mS cm <sup>-1</sup> ) <i>Sp</i> *   <i>Se</i> *	Bulk density (g cm <sup>-3</sup> ) <i>Sp</i> ***   <i>Se</i> **
<i>Avicennia</i>	Wet	13	6.2 ± 0.2 (6.2)	13.4 ± 3.6 (12.9)	0.3 ± 0.1 (0.4)
<i>Avicennia</i>	Dry	5	6.2 ± 0.2 (6.1)	13.9 ± 3.3 (12.2)	0.6 ± 0.2 (0.7)
<i>Rhizophora</i>	Wet	21	6.0 ± 0.4 (6.0)	10.8 ± 2.2 (10.7)	0.5 ± 0.1 (0.4)
<i>Rhizophora</i>	Dry	8	6.0 ± 0.1 (5.9)	13.6 ± 2.4 (13.5)	0.6 ± 0.1 (0.6)

365

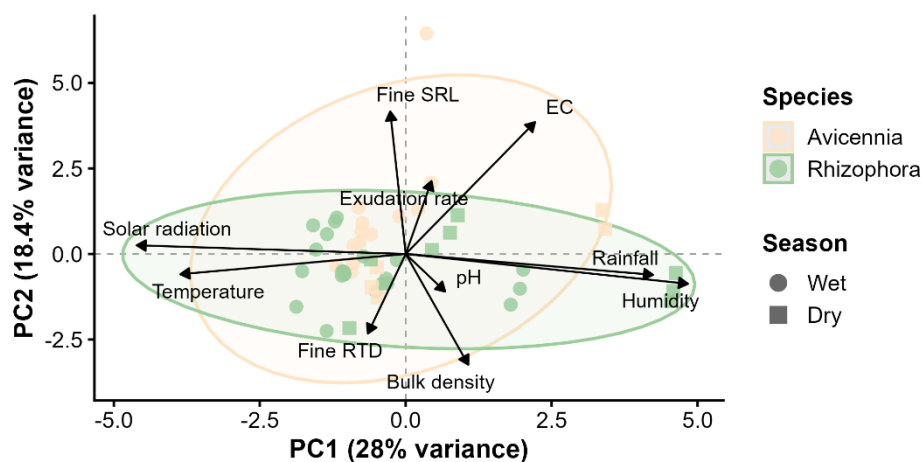
Values shown as mean ± standard deviation (median). EC = electrical conductivity; BD = bulk density. Significance stars in column headers denote species (*Sp*) and season (*Se*) effects. Species effects: pH  $t_{45} = 2.55$ ,  $p = 0.014^*$ ; EC  $t_{45} = 2.23$ ,  $p = 0.031^*$ ; BD  $W = 87$ ,  $p < 0.001^{***}$ ,  $r = -0.67$ . Season effects: pH  $p = 0.91$  (ns); EC  $W = 130$ ,  $p = 0.031^*$ ; BD  $W = 95$ ,  $p = 0.003^{**}$ ,  $r = -0.57$ . \* $p < 0.05$ , \*\* $p < 0.01$ , \*\*\* $p < 0.001$ .

370

### 3.6 Multivariate patterns in root traits and environmental variables

Spearman correlation analyses revealed no significant relationships between root exudation rates and any of the examined variables (Appendix A). Principal component analysis (PCA) was applied to simultaneously explore the relationships between root traits, soil properties, and climatic variables, and to assess multivariate patterns across species and seasons (Fig. 7). PC1 explained 28% of the variance and primarily reflected a climatic gradient, with negative loadings for temperature and solar radiation, and positive loadings for rainfall, humidity, and EC. PC2 explained 18.4% of the variance, and represented a root gradient, with positive loadings for fine root SRL and negative loadings for fine root RTD. Wet season samples (circles) clustered toward negative PC1 values, whereas dry season samples (squares) shifted toward positive PC1 values. Confidence ellipses for *Avicennia* and *Rhizophora* overlapped substantially across both axes. The exudation rate (vector) showed weak associations with the principal components.

380



385 **Figure 7: Principal component analysis of environmental, root trait, and exudation rate variation. The biplot displays all 48-hour incubation samples coloured by species (*Avicennia alba*, beige; *Rhizophora apiculata*, green) and shaped by season (wet season, circles; dry season, squares). PC1 (28% of variance) and PC2 (18.4% of variance) are shown. Confidence ellipses (95%) are drawn per species. Arrows indicate variable loadings for root traits (fine root RTD,  $\text{g cm}^{-3}$ ; fine root SRL,  $\text{m g}^{-1}$ ), soil properties (bulk density,  $\text{g cm}^{-3}$ ; pH; EC,  $\text{mS cm}^{-1}$ ), climatic variables (mean temperature,  $^{\circ}\text{C}$ ; solar radiation,  $\text{kWh}$ ; rainfall,  $\text{mm}$ ; mean humidity, %), and root exudation rate ( $\mu\text{g C g}^{-1} \text{h}^{-1}$ ).**

### 3.7 Ecosystem-scale root exudation fluxes

390 Fine-root exudation from the wet season dataset was upscaled to the soil and ecosystem level using fine-root biomass densities measured in the upper 30 cm of soil. In *Avicennia*-dominated sites ( $n = 13$ ), yearly areal fluxes averaged  $586 \text{ mg C m}^{-2} \text{ day}^{-1}$  (median = 142; SD = 1144). This corresponded to a mean annual flux of  $2140 \text{ kg C ha}^{-1} \text{ yr}^{-1}$  (median = 519  $\text{kg C ha}^{-1} \text{ yr}^{-1}$ ; SD = 4175  $\text{kg C ha}^{-1} \text{ yr}^{-1}$ ). *Rhizophora*-dominant sites ( $n = 21$ ) showed mean daily fluxes of  $299 \text{ mg C m}^{-2} \text{ day}^{-1}$  (median = 144; SD = 433), yielding a mean annual flux of  $1093 \text{ kg C ha}^{-1} \text{ yr}^{-1}$  (median = 526  $\text{kg C ha}^{-1} \text{ yr}^{-1}$ ; SD = 1581  $\text{kg C ha}^{-1} \text{ yr}^{-1}$ ).

395

## 4 Discussion

These results validate the sealed-cuvette method. It has proven to be capable of quantifying root exudation under flooded and waterlogged field conditions, performing robustly across tidally-influenced mangrove soils in a typical tropical carbon-rich mangrove. With an average of  $90.5 \mu\text{g C g}^{-1} \text{h}^{-1}$  (median = 41.1; SD = 132), the C n Gi r mangrove root exudation rates

400 concur with global terrestrial averages (Chari et al., 2024). When combined with fine-root biomass measurements, the root exudation flux was  $1493 \text{ kg C ha}^{-1} \text{ yr}^{-1}$  (median = 522; SD = 2849) in the wet season. This is considerable compared to other fluxes (Adame et al., 2024), demonstrating the importance of root exudation flux integration into mangrove carbon budgets.



#### 4.1 Performance and reliability of the sealed-cuvette system

405 Validating the sealed cuvette method extends cuvette methodology beyond upland terrestrial systems, where it has been  
more extensively applied to quantify root exudation (Gao et al., 2024; Shen et al., 2020; Tückmantel et al., 2017). As  
waterproofing was generally successful in both laboratory and field deployments, our results show that the adaptation we  
introduced to the cuvette design of Phillips et al. (2008) overcame the waterlogged and tidally influenced conditions of  
coastal wetlands. This builds on Kato et al. (2026), whose cuvette was neither sealed against water ingress and light  
penetration, nor buried under sediment, nor did it utilise glass beads. Our approach extends *in situ* root exudation  
410 measurements to more tidally challenging mangrove conditions, while providing the first validation of the approach under  
field conditions.

Although occasional signs of water ingress into the box were observed, these did not correspond to elevated DOC values,  
and occasional high DOC readings did not coincide with visible contamination. Although undetected contamination cannot  
be fully excluded, similar variability has been reported in other cuvette studies, including in mangroves (Kato et al., 2026)  
415 and likely reflects natural heterogeneity in root activity rather than methodological noise (Meier et al., 2020; Phillips et al.,  
2008). DOC recovered from cuvettes containing roots was significantly higher than in controls (Fig. 3), which showed low  
and stable background values as seen in other studies (Phillips et al., 2008, 2011; Shen et al., 2020). The DOC concentrations  
of samples were blank corrected by subtracting the mean of control cuvettes per quadrat, resulting in only two negative  
values in the 48 h dataset, which were removed prior to further analysis. This confirms that background DOC contributions  
420 were minimal and that the sealed chamber effectively isolated root-derived carbon.

The pilot time series revealed a biphasic pattern, with DOC rising over the first 48 hours and declining by 72 hours (Fig. 4).  
This pattern is consistent with previous observations that uprooting initially reduces exudation until roots re-equilibrate,  
whereas extended incubation can lead to root senescence and underestimation of exudation (Oburger and Jones, 2018).  
These findings should nonetheless be interpreted with caution: the pilot time series relied on only three roots, and the overall  
425 effect, while significant, was not supported by significant pairwise differences, limiting the conclusions that can be drawn by  
the time series alone. The primary justification for the 48 h incubation therefore comes from the main dataset, which showed  
no significant difference in root exudation between paired 24- and 48-hour incubations (Fig. 5a), indicating that both  
durations capture comparable mean exudation. Yet Lin's concordance correlation coefficient (Fig. 5b) revealed that  
variability was consistently higher at 24 h, suggesting that some roots may not have fully stabilised within the first day after  
430 excavation. This increased variability supports the idea that roots require a short recovery period after disturbance (Döll et  
al., 2024; Oburger and Jones, 2018). Similarly, prolonged incubations risk senescence (Oburger and Jones, 2018), which  
when coupled with the need to fit tidal access windows while capturing a complete diurnal cycle in exudation, suggests the  
use of a 48 h total protocol (24 h recovery + 24 h effective incubation). We believe this is a physiologically defensible and  
logistically robust basis for *in situ* measurements in wetland soils, and the results may contribute to the limited but growing



435 measurements on exudation in wetland soils (Haviland and Noyce, 2024; Kato et al., 2026; Sasse et al., 2020; Wu et al., 2012; Zhai et al., 2013).

#### 4.2 Root exudation rates in C  n Gi  r

Mangrove root exudation rates in C  n Gi  r ranged from 0.69 to 513.22  $\mu\text{g C g}^{-1} \text{ h}^{-1}$ , with a mean of  $90.5 \pm 132 \mu\text{g C g}^{-1} \text{ h}^{-1}$ . These values fall within a similar range to those reported for upland terrestrial ecosystems (25–140  $\mu\text{g C g}^{-1} \text{ h}^{-1}$ , interquartile  
440 range; Chari et al., 2024), and *Bruguiera gymnorhiza* (L.) Lam. mangrove forests (10–970  $\mu\text{g C g}^{-1} \text{ h}^{-1}$ ; Kato et al., 2026). The average root exudation for *Avicennia* and *Rhizophora* combined was less than half of the exudation rate in the *Bruguiera gymnorhiza* subtropical mangrove forest (mean:  $220 \pm 30 \mu\text{g C g}^{-1} \text{ h}^{-1}$ ; Kato et al., 2026); likely due to a combination of methodological and biological differences (see sections 4.1 and 4.3 respectively).

Exudation rates did not differ significantly between *Avicennia*-dominated stands and *Rhizophora*-dominated stands, nor  
445 between wet and dry seasons (Fig. 6). This non-significance could reflect a genuine absence of biological differences between treatments, insufficient contrast in the underlying drivers (explored in Sect. 4.3), or limited statistical power stemming from the unbalanced and modest sample sizes. However, the modest effect sizes suggest that greater replication alone would be unlikely to reveal a significant difference.

Instead, exudation varied primarily within species and zones rather than between them, with large individual-level variation  
450 comparable to previous cuvette studies (Kato et al., 2026; Meier et al., 2020; Phillips et al., 2008). This within-group variability is consistent with real biological heterogeneity among individual roots, rather than methodological noise: root cuvettes recovered significantly more DOC than blank controls (Fig. 3), confirming that the method reliably captures root-derived carbon at the individual root scale.

#### 4.3 Environmental and root trait drivers of exudation variability

455 To explore which variables drive exudation rates, we applied Spearman correlation analyses between root exudation rates and root traits, soil properties, and climatic variables (Appendix A), which revealed no significant relationships between exudation rate and any of the examined variables. The most likely explanation is that biologically relevant variables, particularly soil nutrient availability and porewater redox conditions which showed positive correlation in sub-tropical mangroves (Kato et al., 2026), were not characterised in this study. In mangrove systems in particular, we suspect hydrology  
460 plays a central role, as higher inundation intensity can enhance soil anoxia and sulphide accumulation, increasing root maintenance costs and potentially suppressing exudation (Kristensen et al., 2008; Zhou et al., 2024). The range of conditions sampled across species and seasons may not have been sufficiently contrasted in order to reveal driver–response relationships.

A PCA integrating root traits, soil properties, and climatic variables (Fig. 7) was consistent with this interpretation: the  
465 exudation rate vector was short and weakly associated with PC1, confidence ellipses for *Avicennia* and *Rhizophora* overlapped substantially across both axes, and together PC1 and PC2 explained only 46.4% of total variance, suggesting that



the sampled conditions were not strongly differentiated. Nonetheless, the PCA did reveal structured variation along two interpretable axes. PC1 reflected a seasonal environmental gradient, with wet-season samples clustering toward negative values and dry-season samples shifting toward positive values, driven by contrasts in rainfall, humidity, and electrical conductivity. PC2 captured a root economic spectrum opposing high SRL against high RTD, consistent with the trade-off between acquisitive and conservative root strategies (Reich, 2014). Though SRL did not differ significantly between species (Table 2), SRL did increase and RTD decreased in the wet season, indicating a shift toward finer, less dense roots under wetter conditions, a pattern shared across both species. Yet this morphological change was not accompanied by elevated exudation rates, suggesting that SRL alone is a poor predictor of exudation in these mangroves, contrary to patterns reported in terrestrial systems (Meier et al., 2020; Tückmantel et al., 2017). Along the seasonal and environmental axis, environmental measurements likewise showed that the underlying ecological contrasts across zones and seasons were small, limiting the potential for divergence of exudation rate between species and seasons. Soils beneath *Avicennia* showed higher pH and electrical conductivity but lower bulk density than beneath *Rhizophora*, and EC and bulk density were both elevated in the dry season. These differences were modest in magnitude.

Taken together, the correlation and ordination analyses suggest that exudation variability in this system is not well explained by the variables measured here, and no strong mechanistic conclusions can be drawn from our data. Although total exudation rates did not differ significantly between species or seasons, it is possible that the *composition* of root exudates varies. Future work incorporating molecular characterisation of exudate composition would help resolve whether the two species and seasons differ functionally even when total flux does not. Identifying the proximal drivers of exudation in mangroves will likely require sampling across more contrasting conditions, including different inundation classes, geomorphological settings, and mangrove species, to determine whether the absence of strong environmental control observed here is a general feature of mangrove exudation, or an artefact of the relatively homogeneous conditions in this study.

#### 4.4 Ecosystem-scale exudation fluxes and carbon budget implications

This study observed that *Avicennia* stands supported greater fine-root biomass than *Rhizophora*, and this structural difference translated into higher ecosystem-scale exudation fluxes: mean annual inputs were approximately 2140 kg C ha<sup>-1</sup> yr<sup>-1</sup> in *Avicennia*-dominant plots and 1093 kg C ha<sup>-1</sup> yr<sup>-1</sup> in *Rhizophora*-dominant plots. Relative to a global mean mangrove GPP of 16–20 Mg C ha<sup>-1</sup> yr<sup>-1</sup> (Adame et al., 2024), fine-root exudation amounted to ~11.9% of GPP in *Avicennia*-dominant plots and ~6.1% in *Rhizophora*-dominant plots, both falling within the range reported across terrestrial ecosystems (Chari et al., 2024). Our measured fluxes are lower than those reported by Kato et al. (2026) for *Bruguiera gymnorhiza*, though direct comparison is complicated by methodological and biological differences between the two studies. Importantly, both studies sampled only to a fraction of the full rooting depth, 30 cm here and 60 cm in Kato et al. (2026); whereas mangrove fine roots extend considerably deeper (Arnaud et al., 2021; Muhammad-Nor et al., 2019). Both estimates are therefore conservative, and the true ecosystem-scale flux is likely higher than reported here.



#### 4.5 Limitations and future directions

500 Several methodological limitations also warrant consideration. A key constraint common to all cuvette-based approaches is  
that isolated fine roots are removed from their natural rhizosphere context, including its microbial community and porewater  
505 chemistry, which may alter exudation rates relative to undisturbed conditions (Oburger and Jones, 2018). This effect is  
reduced by using porewater-like saline solution, glass beads and optimising incubation, and cuvette-based approaches remain  
among the most reliable and widely used methods to quantify exudation under semi-natural conditions (Oburger and Jones,  
2018).

A further limitation concerns the fine-root biomass used for upscaling. Biomass was estimated from only three soil cores per  
quadrat and measured exclusively during the wet season, which likely underrepresents the spatial and temporal variability of  
mangrove root systems. As root biomass directly scales exudation fluxes, this introduces uncertainty into the ecosystem-  
level estimates, which should therefore be interpreted as approximate.

510 An additional constraint is vertical coverage. We sampled exclusively from the upper 30 cm of soil; a depth targeted due to  
high root activity (Arnaud et al., 2023). Yet emerging evidence suggests that this may underestimate total ecosystem  
exudation fluxes. Kato et al. (2026) found that exudation rates in deeper soil layers (30–60 cm) were similar to, and in some  
cases exceeded, those measured at the surface in *Bruguiera gymnorhiza*, with patterns varying across sites and seasons. In a  
temperate beech forest, Tückmantel et al. (2017) reported that exudation rates decline with depth beyond 30 cm,  
515 accompanied by shifts in root morphology. Both confirm that exudation occurs throughout the soil profile, and given that  
mangrove fine roots extend well beyond 30 cm (Arnaud et al., 2021; Muhammad-Nor et al., 2019), our ecosystem-scale flux  
estimates do not capture the variety of exudation along the root profile and should be considered conservative.

Finally, whilst this study provides the first exudation measurements for *Avicennia* and *Rhizophora*, caution is warranted  
when extrapolating these results. Measurements were limited to two species in a single reserve under relatively  
520 homogeneous edaphic conditions; *Avicennia*, for instance, spans a wide range of inundation classes across its global  
distribution, and exudation rates may vary considerably with edaphic context.

These limitations point to clear priorities for future research. Expanding measurements to more contrasting sites,  
encompassing different inundation classes, geomorphological settings, salinity gradients, and mangrove species, is needed to  
identify the environmental drivers of exudation and establish whether the patterns observed here are representative of  
525 tropical mangroves more broadly. The sealed-cuvette approach should also be extended to other coastal wetland types,  
including saltmarshes and tidal freshwater wetlands, where root exudation remains equally unquantified. Beyond bulk  
carbon fluxes, the method is also compatible with compound-level exudate characterisation; applying molecular or  
metabolomic analyses across a range of systems would help resolve whether species and seasonal differences in exudate  
composition exist even where total flux does not and would better constrain the role of root exudates in wetland carbon and  
530 nutrient cycling.

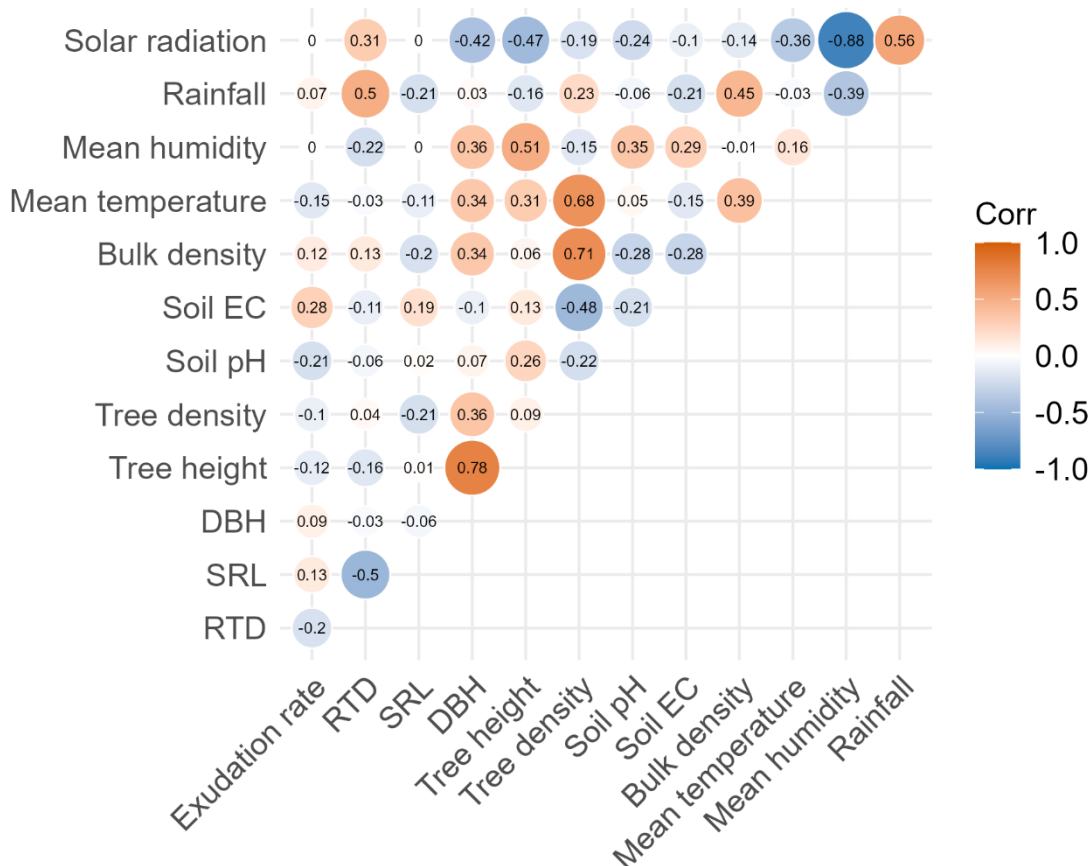


## 5 Conclusions

Overall, this study demonstrates that the sealed cuvette method provides a practical and successful approach for reliable *in situ* quantification of mangrove root exudation under the waterlogged, saline conditions of mangroves, addressing a key methodological limitation in coastal wetland research. The measured average mangrove root exudation rates (mean  $90.5 \pm 132 \mu\text{g C g}^{-1} \text{ h}^{-1}$ ) were in the upper range of terrestrial ecosystem averages (Chari et al., 2024) and showed no significant differences between *Avicennia* and *Rhizophora* or across seasons. When upscaled at the ecosystem level, root exudation was  $1093 \text{ kg C ha}^{-1} \text{ yr}^{-1}$  for *Rhizophora*-dominated plots and  $2140 \text{ kg C ha}^{-1} \text{ yr}^{-1}$  for *Avicennia*-dominated plots which is  $\sim 6.1$  and  $\sim 11.9\%$  of GPP, respectively. Although this study is limited to one mangrove and no clear environmental drivers of exudation were identified, these findings indicate that root exudation represents a meaningful carbon flux that needs to be incorporated into mangrove carbon budgets. Future research can use the work in this study as a basis for helping to expand exudation studies across larger edaphic conditions, to gain a better understanding of root exudation and integrate compositional analyses to better constrain the role of root exudates in mangrove carbon cycling.



545 **Appendix A**



550 **Figure A1: Spearman correlation matrix of root exudation rate and environmental variables measured at 48 h incubations. Circle size and colour indicate the strength and direction of the correlation (orange = positive, blue = negative). RTD = root tissue density ( $\text{g cm}^{-3}$ ); SRL = specific root length ( $\text{m g}^{-1}$ ); DBH = diameter at breast height (cm); Soil EC = electrical conductivity ( $\text{mS cm}^{-1}$ ); Bulk density ( $\text{g cm}^{-3}$ ); Mean temperature ( $^{\circ}\text{C}$ ); Mean humidity (%); Rainfall (mm); Solar radiation ( $\text{W m}^{-2}$ ).  $n = 47$ .**

**Code and data availability**

The data used in this study are available from Zenodo at <https://doi.org/10.5281/zenodo.19361685> and will be made publicly accessible upon publication.

**Author contributions**

555 LH and MA conceived the study. LH developed the sealed-cuvette system, conducted fieldwork, performed formal analysis, curated the data, developed software, and led visualization and manuscript writing. LM contributed to field sampling, data curation, and methodological development. HTD, TL, and NTKB provided resources and supported field sampling and site

access in Càn Giò. HTD, HH, CR, and MA contributed to methodological development. MA, HTD, HH, CR, FD-G, and YG supervised the project. Funding was acquired by MA, CR and FD-G. Validation of results was performed by MA. All authors contributed to writing, review, and editing of the final manuscript.

560

### Competing interests

The authors declare that they have no competing interests.

### Disclaimer

Copernicus Publications remains neutral with regard to jurisdictional claims made in the text, published maps, institutional affiliations, or any other geographical representation in this paper. While Copernicus Publications makes every effort to include appropriate place names, the final responsibility lies with the authors. Views expressed in the text are those of the authors and do not necessarily reflect the views of the publisher.

565

### Acknowledgements

We thank the Càn Giò Mangrove Biosphere Reserve Management Board for site access and logistical support. We are grateful to the students of VNU HCMC for their field assistance.

570

### Financial support

This research has been supported by the TROPECOS project of the exploratory PEPR FairCarboN, managed by the French National Research Agency under the France 2030 programme (grant no. ANR-22-PEXF-012). Additional support was provided by Master thesis grants from the Erasmus Mundus Joint Master Degree in Tropical Biodiversity and Ecosystems – TROPIMUNDO (grant no. 2019-1451), and by H2O'Lyon.

575

### References

Adame, M. F., Cormier, N., Taillardat, P., Iram, N., Rovai, A., Sloey, T. M., Yando, E. S., Blanco-Libreros, J. F., Arnaud, M., Jennerjahn, T., Lovelock, C. E., Friess, D., Reithmaier, G. M. S., Buelow, C. A., Muhammad-Nor, S. M., Twilley, R. R., and Ribeiro, R. A.: Deconstructing the mangrove carbon cycle: Gains, transformation, and losses, *Ecosphere*, 15, e4806, <https://doi.org/10.1002/ecs2.4806>, 2024.

580

Arnaud, M.: Belowground carbon and hydrological dynamics of mangrove forests, Doctor of Philosophy, University of Leeds, 2020.



- Arnaud, M., Morris, P. J., Baird, A. J., Dang, H., and Nguyen, T. T.: Fine root production in a chronosequence of mature reforested mangroves, *New Phytol.*, 232, 1591–1602, <https://doi.org/10.1111/nph.17480>, 2021.
- 585 Arnaud, M., Krause, S., Norby, R. J., Dang, T. H., Acil, N., Kettridge, N., Gauci, V., and Ullah, S.: Global mangrove root production, its controls and roles in the blue carbon budget of mangroves, *Glob. Change Biol.*, 29, 3256–3270, <https://doi.org/10.1111/gcb.16701>, 2023.
- Badri, D. V. and Vivanco, J. M.: Regulation and function of root exudates, *Plant Cell Environ.*, 32, 666–681, <https://doi.org/10.1111/j.1365-3040.2009.01926.x>, 2009.
- 590 Binh, T. T. H., Hoa, P. V., and Nguyen, V. L.: Using Multi-temporal remote sensing data to manage the mangrove for coastal environmental protection, *Int. Arch. Photogramm. Remote Sens. Spat. Inf.*, 37(B8), 709–712, 2008.
- Brauner, K., Birami, B., Brauner, H. A., and Heyer, A. G.: Diurnal periodicity of assimilate transport shapes resource allocation and whole-plant carbon balance, *Plant J.*, 94, 776–789, <https://doi.org/10.1111/tpj.13898>, 2018.
- Chari, N. R., Tumber-Dávila, S. J., Phillips, R. P., Bauerle, T. L., Brunn, M., Hafner, B. D., Klein, T., Obersteiner, S., Reay, M. K., Ullah, S., and Taylor, B. N.: Estimating the global root exudate carbon flux, *Biogeochemistry*, 167, 895–908, <https://doi.org/10.1007/s10533-024-01161-z>, 2024.
- Dijkstra, F. A., Zhu, B., and Cheng, W.: Root effects on soil organic carbon: a double-edged sword, *New Phytol.*, 230, 60–65, <https://doi.org/10.1111/nph.17082>, 2021.
- 600 Döll, S., Koller, H., and Van Dam, N. M.: A simple, cost-effective and optimized protocol for collecting root exudates from soil grown plants, *Rhizosphere*, 30, 100899, <https://doi.org/10.1016/j.rhisph.2024.100899>, 2024.
- Dung, L. V., Tue, N. T., Nhuan, M. T., and Omori, K.: Carbon storage in a restored mangrove forest in Can Gio Mangrove Forest Park, Mekong Delta, Vietnam, *For. Ecol. Manag.*, 380, 31–40, <https://doi.org/10.1016/j.foreco.2016.08.032>, 2016.
- Finzi, A. C., Abramoff, R. Z., Spiller, K. S., Brzostek, E. R., Darby, B. A., Kramer, M. A., and Phillips, R. P.: Rhizosphere processes are quantitatively important components of terrestrial carbon and nutrient cycles, *Glob. Change Biol.*, 21, 2082–2094, <https://doi.org/10.1111/gcb.12816>, 2015.
- 605 Freschet, G. T., Pagès, L., Iversen, C. M., Comas, L. H., Rewald, B., Roumet, C., Klimešová, J., Zadworny, M., Poorter, H., Postma, J. A., Adams, T. S., Bagniewska-Zadworna, A., Bengough, A. G., Blancaflor, E. B., Brunner, I., Cornelissen, J. H. C., Garnier, E., Gessler, A., Hobbie, S. E., Meier, I. C., Mommer, L., Picon-Cochard, C., Rose, L., Ryser, P., Scherer-Lorenzen, M., Soudzilovskaia, N. A., Stokes, A., Sun, T., Valverde-Barrantes, O. J., Weemstra, M., Weigelt, A., Wurzbürger, N., York, L. M., Batterman, S. A., Gomes de Moraes, M., Janeček, Š., Lambers, H., Salmon, V., Tharayil, N., and McCormack, M. L.: A starting guide to root ecology: strengthening ecological concepts and standardising root classification, sampling, processing and trait measurements, *New Phytol.*, 232, 973–1122, <https://doi.org/10.1111/nph.17572>, 2021.
- 610 Gao, Y., Wang, H., Yang, F., Dai, X., Meng, S., Hu, M., Kou, L., and Fu, X.: Relationships between root exudation and root morphological and architectural traits vary with growing season, *Tree Physiol.*, 44, tpad118, <https://doi.org/10.1093/treephys/tpad118>, 2024.
- Haviland, K. A. and Noyce, G. L.: Assessing root–soil interactions in wetland plants: root exudation and radial oxygen loss, *Biogeosciences*, 21, 5185–5198, <https://doi.org/10.5194/bg-21-5185-2024>, 2024.



- 620 Jones, D. L., Hodge, A., and Kuzyakov, Y.: Plant and mycorrhizal regulation of rhizodeposition, *New Phytol.*, 163, 459–480, <https://doi.org/10.1111/j.1469-8137.2004.01130.x>, 2004.
- Jones, D. L., Nguyen, C., and Finlay, R. D.: Carbon flow in the rhizosphere: carbon trading at the soil–root interface, *Plant Soil*, 321, 5–33, <https://doi.org/10.1007/s11104-009-9925-0>, 2009.
- Kato, N., Osaka, K., Ohtsuka, T., and Iimura, Y.: Root exudates in mangrove forests accelerate bicarbonate production in the soil environment, *Sci. Rep.*, 14, 31765, <https://doi.org/10.1038/s41598-024-82873-y>, 2024.
- 625 Kato, N., Osaka, K., Yimatsa, N., Ohtsuka, T., and Iimura, Y.: In Situ Quantification of Root Exudates in a Subtropical Mangrove (*Bruguiera gymnorhiza*) Forest, *Forests*, 17, 156, <https://doi.org/10.3390/f17020156>, 2026.
- Keiluweit, M., Bougoure, J. J., Nico, P. S., Pett-Ridge, J., Weber, P. K., and Kleber, M.: Mineral protection of soil carbon counteracted by root exudates, *Nat. Clim. Change*, 5, 588–595, <https://doi.org/10.1038/nclimate2580>, 2015.
- Kristensen, E., Bouillon, S., Dittmar, T., and Marchand, C.: Organic carbon dynamics in mangrove ecosystems: A review, *Aquat. Bot.*, 89, 201–219, <https://doi.org/10.1016/j.aquabot.2007.12.005>, 2008.
- 630 Krüger, N., Jaishree Subrahmaniam, H., and Mueller, P.: Root exudate profiles of wetland plants - a quantitative synthesis of secretion rates, *Rhizosphere*, 37, 101292, <https://doi.org/10.1016/j.rhisph.2026.101292>, 2026.
- Lin, L. I.-K.: A Concordance Correlation Coefficient to Evaluate Reproducibility, *Biometrics*, 45, 255–268, <https://doi.org/10.2307/2532051>, 1989.
- 635 Lopez-Guerrero, M. G., Wang, P., Phares, F., Schachtman, D. P., Alvarez, S., and Van Dijk, K.: A glass bead semi-hydroponic system for intact maize root exudate analysis and phenotyping, *Plant Methods*, 18, 25, <https://doi.org/10.1186/s13007-022-00856-4>, 2022.
- McIver, J. K., Cope, W. G., Bringolf, R. B., Kwak, T. J., Watson, B., Maynard, A., and Mair, R.: Assessing the Toxicity of Sea Salt to Early Life Stages of Freshwater Mussels: Implications for Sea Level Rise in Coastal Rivers, *Environ. Toxicol. Chem.*, 42, 2478–2489, <https://doi.org/10.1002/etc.5731>, 2023.
- 640 Meier, I. C., Tückmantel, T., Heitkötter, J., Müller, K., Preusser, S., Wrobel, T. J., Kandeler, E., Marschner, B., and Leuschner, C.: Root exudation of mature beech forests across a nutrient availability gradient: the role of root morphology and fungal activity, *New Phytol.*, 226, 583–594, <https://doi.org/10.1111/nph.16389>, 2020.
- Muhammad-Nor, S. M., Huxham, M., Salmon, Y., Duddy, S. J., Mazars-Simon, A., Mencuccini, M., Meir, P., and Jackson, G.: Exceptionally high mangrove root production rates in the Kelantan Delta, Malaysia; An experimental and comparative study, *For. Ecol. Manag.*, 444, 214–224, <https://doi.org/10.1016/j.foreco.2019.04.026>, 2019.
- 645 Oburger, E. and Jones, D. L.: Sampling root exudates – Mission impossible?, *Rhizosphere*, 6, 116–133, <https://doi.org/10.1016/j.rhisph.2018.06.004>, 2018.
- OpenStreetMap contributors: <https://www.openstreetmap.org>, (last access: October 2025), 2025.
- 650 Panchal, P., Preece, C., Peñuelas, J., and Giri, J.: Soil carbon sequestration by root exudates, *Trends Plant Sci.*, 27, 749–757, <https://doi.org/10.1016/j.tplants.2022.04.009>, 2022.



- Phillips, R. P., Erlitz, Y., Bier, R., and Bernhardt, E. S.: New approach for capturing soluble root exudates in forest soils, *Funct. Ecol.*, 22, 990–999, <https://doi.org/10.1111/j.1365-2435.2008.01495.x>, 2008.
- 655 Phillips, R. P., Finzi, A. C., and Bernhardt, E. S.: Enhanced root exudation induces microbial feedbacks to N cycling in a pine forest under long-term CO<sub>2</sub> fumigation, *Ecol. Lett.*, 14, 187–194, <https://doi.org/10.1111/j.1461-0248.2010.01570.x>, 2011.
- Posit Team: *RStudio: Integrated Development Environment for R*, Posit Software, PBC, Boston, MA, 2024.
- QGIS Development Team: QGIS Geographic Information System, Open Source Geospatial Foundation [code], <https://qgis.org>, 2025.
- 660 Reich, P. B.: The world-wide ‘fast–slow’ plant economics spectrum: a traits manifesto, *J. Ecol.*, 102, 275–301, <https://doi.org/10.1111/1365-2745.12211>, 2014.
- Robert, C. A. M., Himmighofen, P., McLaughlin, S., Cofer, T. M., Khan, S. A., Siffert, A., and Sasse, J.: Environmental and Biological Drivers of Root Exudation, *Annu. Rev. Plant Biol.*, 76, 317–339, <https://doi.org/10.1146/annurev-arplant-083123-082752>, 2025.
- 665 R Core Team: *R: A language and environment for statistical computing*, R Foundation for Statistical Computing, Vienna, Austria, 2024.
- Sasse, J., Kosina, S. M., De Raad, M., Jordan, J. S., Whiting, K., Zhalnina, K., and Northen, T. R.: Root morphology and exudate availability are shaped by particle size and chemistry in *Brachypodium distachyon*, *Plant Direct*, 4, e00207, <https://doi.org/10.1002/pld3.207>, 2020.
- 670 Shen, X., Yang, F., Xiao, C., and Zhou, Y.: Increased contribution of root exudates to soil carbon input during grassland degradation, *Soil Biol. Biochem.*, 146, 107817, <https://doi.org/10.1016/j.soilbio.2020.107817>, 2020.
- Tixier, A., Forest, M., Prudent, M., Durey, V., Zwieniecki, M., and Barnard, R. L.: Root exudation of carbon and nitrogen compounds varies over the day-night cycle in pea: The role of diurnal changes in internal pools, *Plant Cell Environ.*, 46, 962–974, <https://doi.org/10.1111/pce.14523>, 2023.
- 675 Tückmantel, T., Leuschner, C., Preusser, S., Kandeler, E., Angst, G., Mueller, C. W., and Meier, I. C.: Root exudation patterns in a beech forest: Dependence on soil depth, root morphology, and environment, *Soil Biol. Biochem.*, 107, 188–197, <https://doi.org/10.1016/j.soilbio.2017.01.006>, 2017.
- UNESCO /MAB Project: Valuation of the Mangrove Ecosystem in Can Gio Biosphere Reserve, Vietnam. Final Report. Implemented by: The Vietnam MAB National Committee, Hanoi, 2000.
- 680 Van Loon, A. F., Dijkema, R., and Van Mensvoort, M. E. F.: Hydrological classification in mangrove areas: A case study in Can Gio, Vietnam, *Aquat. Bot.*, 87, 80–82, <https://doi.org/10.1016/j.aquabot.2007.02.001>, 2007.
- Van Vinh, T., Marchand, C., Linh, T. V. K., Jacotot, A., Nho, N. T., and Allenbach, M.: Soil and Aboveground Carbon Stocks in a Planted Tropical Mangrove Forest (Can Gio, Vietnam), in: *Wetland Carbon and Environmental Management*, American Geophysical Union (AGU), 229–245, <https://doi.org/10.1002/9781119639305.ch12>, 2021.



- 685 Visual Crossing: Weather API [data service], <https://www.visualcrossing.com/weather-api/>, last access: 6 March 2025.
- Vives-Peris, V., De Ollas, C., Gómez-Cadenas, A., and Pérez-Clemente, R. M.: Root exudates: from plant to rhizosphere and beyond, *Plant Cell Rep.*, 39, 3–17, <https://doi.org/10.1007/s00299-019-02447-5>, 2020.
- Williams, A., Langridge, H., Straathof, A. L., Fox, G., Muhammadali, H., Hollywood, K. A., Xu, Y., Goodacre, R., and de Vries, F. T.: Comparing root exudate collection techniques: An improved hybrid method, *Soil Biol. Biochem.*, 161, 108391, <https://doi.org/10.1016/j.soilbio.2021.108391>, 2021.
- 690 Wilson, S. D.: Below-ground opportunities in vegetation science, *J. Veg. Sci.*, 25, 1117–1125, <https://doi.org/10.1111/jvs.12168>, 2014.
- Wu, F. Y., Chung, A. K. C., Tam, N. F. Y., and Wong, M. H.: Root exudates of wetland plants influenced by nutrient status and types of plant cultivation, *Int. J. Phytoremediation*, 14, 543–553, <https://doi.org/10.1080/15226514.2011.604691>, 2012.
- 695 Zhai, X., Piwpuan, N., Arias, C. A., Headley, T., and Brix, H.: Can root exudates from emergent wetland plants fuel denitrification in subsurface flow constructed wetland systems?, *Ecol. Eng.*, 61, 555–563, <https://doi.org/10.1016/j.ecoleng.2013.02.014>, 2013.
- Zhou, L., Li, X., Hao, S., Hong, L., Chen, L., and Li, Q. Q.: Distinct molecular responses of mangrove plants to hypoxia and reoxygenation stresses contribute to their resilience in coastal wetland environment, *Sci. Total Environ.*, 956, 177357, <https://doi.org/10.1016/j.scitotenv.2024.177357>, 2024.
- 700